Theoretical estimate on tensor-polarization asymmetry in proton-deuteron Drell-Yan process

S. Kumano[1,2,3] and Qin-Tao Song[1,3]

[1]*KEK Theory Center, Institute of Particle and Nuclear Studies, High Energy Accelerator Research Organization (KEK), 1-1, Ooho, Tsukuba, Ibaraki 305-0801, Japan*

[2]*J-PARC Branch, KEK Theory Center, Institute of Particle and Nuclear Studies, KEK, and Theory Group, Particle and Nuclear Physics Division, J-PARC Center, 203-1, Shirakata, Tokai, Ibaraki 319-1106, Japan*

[3]*Department of Particle and Nuclear Physics, Graduate University for Advanced Studies (SOKENDAI), 1-1, Ooho, Tsukuba, Ibaraki 305-0801, Japan*

(Received 9 June 2016; published 20 September 2016)

Tensor-polarized parton distribution functions are new quantities in spin-1 hadrons such as the deuteron, and they could probe new quark-gluon dynamics in hadron and nuclear physics. In charged-lepton deep inelastic scattering, they are studied by the twist-2 structure functions b_1 and b_2. The HERMES Collaboration found unexpectedly large b_1 values compared to a naive theoretical expectation based on the standard deuteron model. The situation should be significantly improved in the near future by an approved experiment to measure b_1 at Thomas Jefferson National Accelerator Facility (JLab). There is also an interesting indication in the HERMES result that finite antiquark tensor polarization exists. It could play an important role in solving a mechanism on tensor structure in the quark-gluon level. The tensor-polarized antiquark distributions are not easily determined from the charged-lepton deep inelastic scattering; however, they can be measured in a proton-deuteron Drell-Yan process with a tensor-polarized deuteron target. In this article, we estimate the tensor-polarization asymmetry for a possible Fermilab Main-Injector experiment by using optimum tensor-polarized parton distribution functions to explain the HERMES measurement. We find that the asymmetry is typically a few percent. If it is measured, it could probe new hadron physics, and such studies could create an interesting field of high-energy spin physics. In addition, we find that a significant tensor-polarized gluon distribution should exist due to Q^2 evolution, even if it were zero at a low Q^2 scale. The tensor-polarized gluon distribution has never been observed, so it is an interesting future project.

DOI: 10.1103/PhysRevD.94.054022

I. INTRODUCTION

It was discovered by the European Muon Collaboration (EMC) in the measurement of the polarized structure function g_1 that only a small fraction of nucleon spin is carried by quarks [1], which is in contradiction to the naive quark model. Since then, many theoretical and experimental efforts have been made to clarify the origin of the nucleon spin. There could be contributions from gluon spin and partonic angular momenta. Theoretical and experimental efforts are in progress to solve the issue.

On the other hand, there are new polarized structure functions [2,3], which do not exist in the spin-1/2 nucleon, for spin-1 hadrons and nuclei such as the deuteron. In charged-lepton deep inelastic scattering, they are named b_1, b_2, b_3, and b_4 [3]. Projection operators of b_{1-4} on the hadron tensor $W_{\mu\nu}$ are obtained in Ref. [4]. The twist-2 functions are b_1 and b_2, and they are related to each other by the Callan-Gross–like relation $2xb_1 = b_2$ in the Bjorken scaling limit. Therefore, it is interesting to investigate the leading-twist b_1 (or b_2) first. A useful sum rule for the twist-2 function b_1 was proposed in Ref. [5] by using the parton model, and it could be used as a guideline for the existence of tensor-polarized antiquark distributions. On the other hand, proton-deuteron Drell-Yan processes are theoretically formulated in Ref. [6] for the polarized deuteron including tensor polarization.

The leading-twist structure function b_1 probes a peculiar aspect of internal structure in a spin-1 hadron. It vanishes if internal constituents are in the S wave, which indicates that it is a suitable observable for probing a dynamical aspect, possibly an exotic one, inside the hadron. In fact, the first measurement of b_1 by the HERMES Collaboration [7] indicated that the magnitude of b_1 is much larger than the one expected by the standard deuteron model with D-state admixture [3,8]. There could be other effects from pions [9] and shadowing phenomena [10] in the deuteron. There is also a suggestion that b_1 studies could lead to a new finding on a hidden-color component [9]. On related spin-1 hadron physics, there are investigations on leptoproduction of the spin-1 hadron [11], fragmentation functions [12], generalized parton distributions [13], target-mass corrections [14], positivity constraints [15], lattice QCD estimate [16], and angular momenta for the spin-1 hadron [17].

The first measurement of b_1 was done by the HERMES Collaboration in 2005 [7]. Its data indicated that b_1 has

interesting oscillatory behavior as the function of x and that the magnitude of xb_1 is of the order of 10^{-3}. Since b_1 is expressed by tensor-polarized parton distribution functions, possible quark and antiquark distributions $[\delta_T q(x), \delta_T \bar{q}(x)]$ were extracted from the HERMES data [18]. The analysis suggested finite tensor-polarized antiquark distributions from the data at $x < 0.1$. Although the sign change of b_1 is expected in a convolution description for the deuteron with D-state admixture, the HERMES data indicate much larger $|b_1|$. Therefore, the b_1 is expected to probe nonconventional physics beyond the standard deuteron model. The HERMES measurement also suggested a new phenomenon on a finite tensor polarization for antiquarks. There is a sum rule for b_1 [5], and a deviation from this sum indicated the finite tensor-polarized antiquark distributions in a way similar to the Gottfried sum-rule violation [19].

The deuteron tensor structure has been investigated for a long time at low energies. However, the time has come to investigate it, through the tensor-polarized structure functions and parton distribution functions, in terms of quark and gluon degrees of freedom. Furthermore, these quantities could be sensitive to exotic features such as the hidden color [9]. In the HERMES measurement, there is already a hint that new hadron physics is needed to interpret its data. Therefore, a new field of high-energy spin physics could be created by investigating the tensor structure functions, as the EMC measurement created the field of high-energy spin physics for the spin-1/2 nucleon. The current situation on b_1 and tensor-polarized parton distribution functions (PDFs) is summarized in Ref. [20].

By considering this prominent prospect, the Thomas Jefferson National Accelerator Facility (JLab) experiment was approved for measuring the structure function b_1 [21], and the actual experiment will start in a few years. In addition, the related tensor polarization A_{zz} can be investigated at JLab in the large-x region [22]. These b_1 and A_{zz} could be also investigated at the future Electron-Ion Collider (EIC) [23].

In a simple model for the deuteron, it is not obvious to have a tensor-polarized antiquark distribution; however, a finite value is indicated in the HERMES experiment for the antiquark tensor polarization. The best way to probe the antiquark distributions is to use a Drell-Yan process with a tensor-polarized deuteron target [6]. The Drell-Yan process for unpolarized proton with tensor-polarized deuteron is possible, and its measurement is now under consideration at Fermilab [24]. However, there is no theoretical estimate on the tensor-polarized spin asymmetry, so it is necessary to show even the order of magnitude for an experimental proposal, especially for considering beam-time allocation in an actual measurement. The purpose of this article is to show expected spin asymmetries for the Fermilab measurement.

In this article, we explain formalisms first in Sec. [18], especially on the tensor-polarized structure functions and PDFs in Sec. II A, and the tensor-polarized Drell-Yan spin asymmetry is expressed in terms of the tensor-polarized PDFs in Sec. [6]. Then, our estimates on the spin asymmetry are shown for the possible Fermilab experiment in Sec. III. The results are summarized in Sec. IV.

II. TENSOR-POLARIZED DISTRIBUTION FUNCTIONS FOR SPIN-1 DEUTERON

We explain basic formalisms involving tensor-polarized structure functions and PDFs in deep inelastic charged-lepton scattering and the proton-deuteron Drell-Yan process.

A. Tensor-polarized structure functions in charged-lepton deep inelastic scattering

First, the charged-lepton deep inelastic scattering (DIS) from the polarized deuteron is explained. The polarized DIS formalism for the charged lepton from the nucleon is well known, and it is generally expressed in terms of four structure functions, F_1, F_2, g_1, and g_2. In addition to these functions, there exist four new structure functions, b_1, b_2, b_3, and b_4, in the DIS from the spin-1 hadron such as the deuteron.

In the charged-lepton DIS shown in Fig. 1, the hadron tensor $W_{\mu\nu}$ is generally expressed for a spin-1 hadron as [3,4,20]

$$\begin{aligned} W_{\mu\nu}^{\lambda_f\lambda_i} &= \frac{1}{4\pi M}\int d^4\xi e^{iq\cdot\xi}\langle p,\lambda_f|[J_\mu^{em}(\xi), J_\nu^{em}(0)]|p,\lambda_i\rangle \\ &= -F_1\hat{g}_{\mu\nu} + \frac{F_2}{M\nu}\hat{p}_\mu\hat{p}_\nu + \frac{ig_1}{\nu}\epsilon_{\mu\nu\lambda\sigma}q^\lambda s^\sigma \\ &\quad + \frac{ig_2}{M\nu^2}\epsilon_{\mu\nu\lambda\sigma}q^\lambda(p\cdot q s^\sigma - s\cdot q p^\sigma) \\ &\quad - b_1 r_{\mu\nu} + \frac{1}{6}b_2(s_{\mu\nu} + t_{\mu\nu} + u_{\mu\nu}) \\ &\quad + \frac{1}{2}b_3(s_{\mu\nu} - u_{\mu\nu}) + \frac{1}{2}b_4(s_{\mu\nu} - t_{\mu\nu}), \end{aligned} \tag{1}$$

by the eight structure functions including the new ones $b_{1\text{–}4}$. Here, the kinematical coefficients $r_{\mu\nu}$, $s_{\mu\nu}$, $t_{\mu\nu}$, and $u_{\mu\nu}$ are defined as

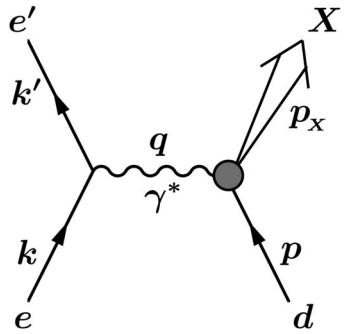

FIG. 1. Deep inelastic scattering of charged lepton (e) from spin-1 hadron d.

$$
\begin{aligned}
r_{\mu\nu} &= \frac{1}{\nu^2}\left[q\cdot E^*(\lambda_f)q\cdot E(\lambda_i) - \frac{1}{3}\nu^2\kappa\right]\hat{g}_{\mu\nu},\\
s_{\mu\nu} &= \frac{2}{\nu^2}\left[q\cdot E^*(\lambda_f)q\cdot E(\lambda_i) - \frac{1}{3}\nu^2\kappa\right]\frac{\hat{p}_\mu\hat{p}_\nu}{M\nu},\\
t_{\mu\nu} &= \frac{1}{2\nu^2}\Big[q\cdot E^*(\lambda_f)\{\hat{p}_\mu\hat{E}_\nu(\lambda_i)+\hat{p}_\nu\hat{E}_\mu(\lambda_i)\}\\
&\quad + \{\hat{p}_\mu\hat{E}^*_\nu(\lambda_f)+\hat{p}_\nu\hat{E}^*_\mu(\lambda_f)\}q\cdot E(\lambda_i) - \frac{4\nu}{3M}\hat{p}_\mu\hat{p}_\nu\Big],\\
u_{\mu\nu} &= \frac{M}{\nu}\Big[\hat{E}^*_\mu(\lambda_f)\hat{E}_\nu(\lambda_i)+\hat{E}^*_\nu(\lambda_f)\hat{E}_\mu(\lambda_i)\\
&\quad + \frac{2}{3}\hat{g}_{\mu\nu} - \frac{2}{3M^2}\hat{p}_\mu\hat{p}_\nu\Big].
\end{aligned}
\tag{2}
$$

In these equations, k and k' are initial and final lepton momenta; M, p, and q are hadron mass, hadron momentum, and momentum transfer; ν and Q^2 are defined by $\nu = p\cdot q/M$ and $Q^2 = -q^2 > 0$; p_X is given by $p_X = p+q$; and $\epsilon_{\mu\nu\lambda\sigma}$ is an antisymmetric tensor with the convention $\epsilon_{0123} = +1$. The notations $\hat{g}_{\mu\nu}$ and $\hat{p}_\mu$ are used for satisfying the current conservation $q^\mu W_{\mu\nu} = q^\nu W_{\mu\nu} = 0$, and they are defined by

$$
\hat{g}_{\mu\nu} \equiv g_{\mu\nu} - \frac{q_\mu q_\nu}{q^2}, \qquad \hat{a}_\mu \equiv a_\mu - \frac{a\cdot q}{q^2}q_\mu. \tag{3}
$$

Furthermore, κ is defined by $\kappa = 1 + Q^2/\nu^2$, s^μ is the spin vector of the spin-1 hadron, and E^μ is the polarization vector of the spin-1 hadron with the constraints, $p\cdot E = 0$ and $E^*\cdot E = -1$. The polarization vector is taken as the spherical unit vectors,

$$
\begin{aligned}
E^\mu(\lambda = \pm 1) &= \frac{1}{\sqrt{2}}(0, \mp 1, -i, 0),\\
E^\mu(\lambda = 0) &= (0,0,0,1),
\end{aligned}
\tag{4}
$$

and its relation to the spin vector is given by

$$
(s_{\lambda_f\lambda_i})^\mu = -\frac{i}{M}\epsilon^{\mu\nu\alpha\beta}E^*_\nu(\lambda_f)E_\alpha(\lambda_i)p_\beta. \tag{5}
$$

In these equations, we explicitly denoted the initial and final spin states by λ_i and λ_f, respectively, because off-diagonal terms with $\lambda_f \neq \lambda_i$ are generally needed to discuss higher-twist contributions [3].

Among the four new structure functions b_{1-4}, b_3 and b_4 are higher-twist functions, and the twist-2 functions b_1 and b_2 are related to each other by the Callan-Gross–like relation $2xb_1 = b_2$ in the Bjorken scaling limit. The functions b_1 and b_2 are expressed by the tensor-polarized parton distribution functions $\delta_T f(x)$ defined by [25]

$$
\delta_T f(x,Q^2) \equiv f^0(x,Q^2) - \frac{f^{+1}(x,Q^2)+f^{-1}(x,Q^2)}{2}, \tag{6}
$$

where f^λ indicates an unpolarized parton distribution in the hadron spin state λ. Using the tensor-polarized quark and antiquark distributions, we have the structure function

$$
b_1(x,Q^2) = \frac{1}{2}\sum_i e_i^2[\delta_T q_i(x,Q^2) + \delta_T\bar{q}_i(x,Q^2)] \tag{7}
$$

in the parton model. Here, e_i is the charge of the quark flavor i.

There is a sum rule for b_1 based on the parton model [5,18], and it is similar to the Gottfried sum rule [19],

$$
\begin{aligned}
\int dx b_1(x) &= -\lim_{t\to 0}\frac{5}{24}tF_Q(t)\\
&\quad + \frac{1}{9}\int dx[4\delta_T\bar{u}(x) + \delta_T\bar{d}(x) + \delta_T\bar{s}(x)],\\
\int \frac{dx}{x}[F_2^p(x) - F_2^n(x)] &= \frac{1}{3} + \frac{2}{3}\int dx[\bar{u}(x) - \bar{d}(x)],
\end{aligned}
\tag{8}
$$

where $F_Q(t)$ is the electric quadrupole form factor for the spin-1 hadron and this first term vanishes: $\lim_{t\to 0}\frac{5}{24}tF_Q(t) = 0$. These relations are derived in the parton model, and they are not rigorous ones obtained, for example, by the current algebra [26]. Therefore, depending on the small-x behavior of $\bar{u}-\bar{d}$ (or $F_2^p - F_2^n$) and $\delta_T\bar{q}$ (or b_1), these sums may diverge although $\bar{u}$ and $\bar{d}$ are currently assumed to be equal at very small x where experimental data do not exist. These sum rules should be considered as guidelines based on the parton model. In any case, as the violation of the Gottfried sum rule created the field of flavor dependence in antiquark distributions and studies of nonperturbative mechanisms behind it, the deviation from zero for the b_1 sum could probe the interesting tensor-polarized antiquark distributions $\delta_T\bar{q}$ and possibly exotic mechanisms behind them as shown in Eq. (8).

The HERMES Collaboration reported the first measurement on b_1 [7], and its data were analyzed to obtain possible tensor-polarized PDFs in Ref. [18]. Since there is little information for the tensor-polarized PDFs at this stage, we need to introduce bold assumptions for extracting the distributions from the experimental data. However, the b_1 seems to have a node at a medium x point. First, a conventional convolution description for b_1 indicates an oscillatory x dependence [3,8]. Namely, it is negative at $x > 0.5$, and it turns into positive at $x < 0.5$. Second, the sign change is also suggested by the HERMES data at $x = 0.2$–0.3. Third, the b_1 sum needs the node to satisfy $\int dx b_1(x) = 0$. From these ideas, we considered that tensor-polarized PDFs for the deuteron are expressed by

the unpolarized PDFs multiplied by a function $\delta_T w(x)$ at Q_0^2 as [18]

$$\begin{aligned}\delta_T q_v^D(x,Q_0^2) &\equiv \delta_T u_v^D(x,Q_0^2) = \delta_T d_v^D(x,Q_0^2) \\ &= \delta_T w(x)\frac{u_v(x,Q_0^2)+d_v(x,Q_0^2)}{2}, \\ \delta_T \bar{q}^D(x,Q_0^2) &\equiv \delta_T \bar{u}^D(x,Q_0^2) = \delta_T \bar{d}^D(x,Q_0^2) \\ &= \delta_T s^D(x,Q_0^2) = \delta_T \bar{s}^D(x,Q_0^2) \\ &= \alpha_{\bar{q}}\delta_T w(x) \\ &\quad \times \frac{2\bar{u}(x,Q_0^2)+2\bar{d}(x,Q_0^2)+s(x,Q_0^2)+\bar{s}(x,Q_0^2)}{6}.\end{aligned} \tag{9}$$

Here, D indicates the deuteron, and the capital letter is used to avoid confusion with a d quark, and the modification function $\delta_T w(x)$ is expressed by a simple polynomial form with a node at $x = x_0$:

$$\delta_T w(x) = a x^b (1-x)^c (x_0 - x). \tag{10}$$

It means that a certain fraction of the unpolarized PDFs is tensor polarized, and this fraction is given by $\delta_T w(x)$ or $\alpha_{\bar{q}}\delta_T w(x)$ for valence-quark and antiquark distributions, respectively. In the analysis of Ref. [18], the scale is taken as the average Q^2 of the HERMES experiment ($Q_0^2 = 2.5$ GeV^2). The parameters a, b, c, and x_0 are determined by a χ^2 analysis of the HERMES data with the leading-order expression for b_1 in Eq. (7) by considering two options:

(1) Set 1: There is no tensor-polarized antiquark distribution at the scale Q_0^2 ($\alpha_{\bar{q}} = 0$).
(2) Set 2: There could be finite tensor-polarized antiquark distributions at the scale Q_0^2 ($\alpha_{\bar{q}}$ is a free parameter).

The determined parameter values are $a = 0.221 \pm 0.174$ (0.378 ± 0.212), $b = 0.648 \pm 0.342$ (0.706 ± 0.324), $\alpha_{\bar{q}} = 3.20 \pm 2.75$ (fixed $= 0$), $c =$ fixed $= 1$ (1), and $x_0 = 0.221$ (0.229) in set 2 (set 1).

Since the error matrix or Hessian is obtained in the χ^2 analysis, it is possible to show an error band for the obtained b_1 curve. The details of the Hessian method are explained elsewhere [27], so a brief outline is explained in the following. Expanding χ^2 around the minimum parameter set $\hat{\xi}$, we have the χ^2 change ($\Delta\chi^2$) expressed by the second derivative matrix H_{ij}, which is called Hessian, as

$$\Delta\chi^2 = \chi^2(\hat{\xi}+\delta\xi) - \chi^2(\hat{\xi}) = \sum_{i,j} H_{ij}\delta\xi_i\delta\xi_j. \tag{11}$$

Then, the error of a physics quantity $f(x)$ is calculated by the Hessian and as

$$[\delta f(x)]^2 = \Delta\chi^2 \sum_{i,j}\left[\frac{\partial f(x)}{\partial\xi_i}\right]_{\hat{\xi}} H_{ij}^{-1}\left[\frac{\partial f(x)}{\partial\xi_j}\right]_{\hat{\xi}}. \tag{12}$$

In the set-2 analysis, there are three parameters $\xi_i = a$, b, and $\alpha_{\bar{q}}$. The node point x_0 is expressed by the parameter b. The derivatives with respect to the parameters ξ_i need to be calculated. As for the $\Delta\chi^2$ value, we may take $\Delta\chi^2 = 1$. However, a larger value ($\Delta\chi^2 \sim N$, $N =$ number of parameters) is often taken in the PDF analyses, and it is called a tolerance. In Ref. [27], one-σ range is given so that the confidence level becomes 68% for the multiparameter normal distribution. For $N = 3$, it is $\Delta\chi^2 = 3.53$. In showing uncertainty bands, we take $\Delta\chi^2 = 1$ and 3.53 in this work. In any case, they are related with each other by changing the band width by the scale $\sqrt{3.53} = 1.88$.

Our optimum structure function b_1 of set 2 is shown in Fig. 2 by the solid curve in comparison with the HERMES data. The set-1 result is shown by the dashed curve, which significantly deviates from the data at small x (<0.1). Although the analysis results depend on the parametrization function, the small-x data cannot be explained if there is no contribution from the tensor-polarized antiquark distributions. Set 2 is a reasonable fit to the experimental measurements. Two uncertainty bands are shown in Fig. 2 by taking $\Delta\chi^2 = 1$ and 3.53. The set-1 curve is in the error-band boundary at $x < 0.1$ by considering the uncertainties, which indicates that the set-1 function could be marginally consistent with the measurements. It is because the errors of the HERMES measurements are large, and hence the function b_1 still has large errors.

Then, the determined tensor-polarized PDFs are shown in Fig. 3. The tensor-polarized valence-quark and antiquark distributions are shown for set 2 by the solid and dotted curves, and the valence-quark distribution of the set 1 is

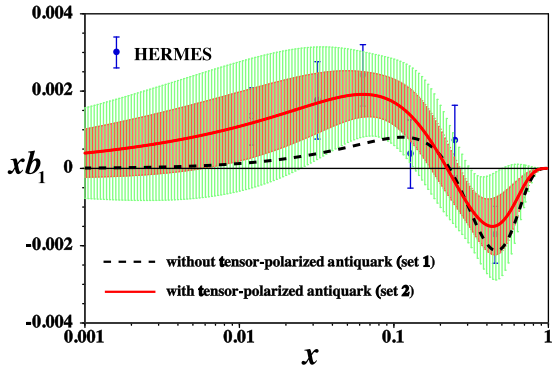

FIG. 2. χ^2 analysis results are compared with HERMES data [7]. The solid and dashed curves indicate theoretical results with finite tensor-polarized antiquark distributions (set 2, $\alpha_{\bar{q}} \neq 0$) and without them (set 1, $\alpha_{\bar{q}} = 0$), respectively. The open circle is the data at $Q^2 < 1$ GeV^2, and it is not included in the fit analysis [18]. The uncertainties of the set-2 curve are shown by the bands with $\Delta\chi^2 = 1$ and 3.53.

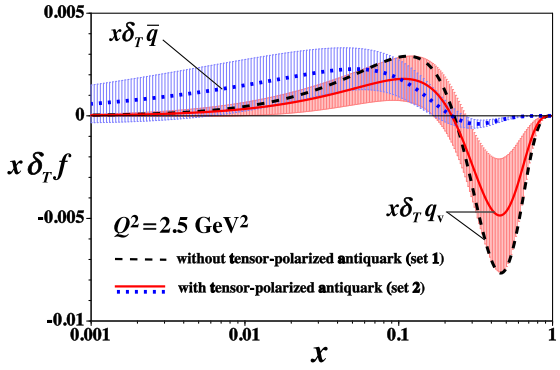

FIG. 3. Obtained tensor-polarized PDFs at $Q^2 = 2.5$ GeV^2. The solid and dashed curves indicate the tensor-polarized valence-quark distributions $x\delta_T q_v(x)$ with finite tensor-polarized antiquark distributions (set 2, $\alpha_{\bar{q}} \neq 0$) and without them (set 1, $\alpha_{\bar{q}} = 0$), respectively. The dotted curve is the tensor-polarized antiquark distribution $x\delta_T \bar{q}(x)$ in set 2 [18]. The uncertainty bands of $\Delta\chi^2 = 1$ are shown.

shown by the dashed curves. All the distributions are negative at large x (>0.2), and they turn into positive at the node point around $x \sim 0.2$. These are distributions at $Q^2 = 2.5$ GeV^2. Since these distributions are the only ones determined by the χ^2 analysis of existing b_1 data in a model-independent way, we use them for estimating the tensor-polarization asymmetry in the proton-deuteron Drell-Yan process at Fermilab. However, one should note that the tensor-polaried PDFs are not determined well at this stage as shown by the error bands in Fig. 3, and future experimental progress is obviously needed for b_1. Only the uncertainty bands of $\Delta\chi^2 = 1$ are shown in Fig. 3. Hereafter, $\Delta\chi^2 = 1$ bands are shown in the figures.

B. Polarized proton-deuteron Drell-Yan process with tensor-polarized deuteron

Polarized proton-proton Drell-Yan processes have been theoretically investigated extensively, and the studies are foundations for the Relativistic Heavy Ion Collider (RHIC)-spin project. However, polarized proton-deuteron processes have not been studied well partly because there was no actual experimental project. In the 1990s, a possible deuteron-beam polarization was considered for the RHIC [28]; however, it was not realized. On the other hand, the polarized proton-deuteron Drell-Yan processes are possible with a polarized deuteron target, and it is becoming a realistic project at Fermilab.

The formalisms of polarized proton-deuteron Drell-Yan processes were investigated in Ref. [6]. The cross section for the Drell-Yan process $p + d \to \mu^+\mu^- + X$ is given by a lepton tensor multiplied by the hadron tensor

$$W_{\mu\nu}^{\rm DY} = \frac{1}{4\pi M}\int d^4\xi e^{-i(k_1+k_2)\cdot\xi}\langle pd|J_\mu^{em}(\xi)J_\nu^{em}(0)|pd\rangle, \quad (13)$$

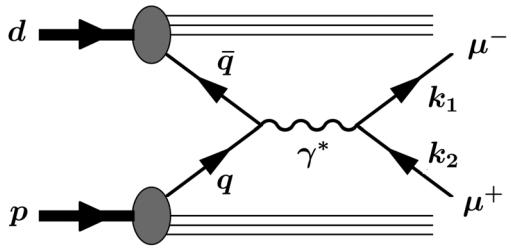

FIG. 4. Typical Drell-Yan process.

where k_1 and k_2 are momenta for μ^- and μ^+, respectively. The leading subprocess, which contributes to the cross section, is the quark-antiquark annihilation process $q\bar{q} \to \mu^+\mu^-$ shown in Fig. 4.

According to the general formalism for $W_{\mu\nu}^{\rm DY}$ by using Hermiticity, parity conservation, and time-reversal invariance [6], there exist 108 structure functions in the proton-deuteron (pd) Drell-Yan processes instead of 48 functions in the proton-proton (pp) Drell-Yan. There are 60 new structure functions due to the spin-1 nature of the deuteron. However, most of them are higher-twist functions, and all of them are not important especially at the first stage. Because it is too lengthy to write these structure functions, we explain only the essential functions associated with the leading-twist part of the deuteron tensor structure.

In the pp Drell-Yan processes, there are spin asymmetries by combinations of the unpolarized state (U) together with longitudinal (L) and transverse (T) polarizations: $\langle\sigma\rangle$, A_{LL}, A_{TT}, A_{LT}, and $A_T(=A_{UT}, A_{TU})$. In the pd Drell-Yan, additional tensor-polarization asymmetries exist, and the spin asymmetries

$$\langle\sigma\rangle,\ A_{LL},\ A_{TT},\ A_{LT},\ A_{TL},\ A_{UT},\ A_{TU},$$
$$A_{UQ_0},\ A_{TQ_0},\ A_{UQ_1},\ A_{LQ_1},\ A_{TQ_1},\ A_{UQ_2},\ A_{LQ_2},\ A_{TQ_2} \quad (14)$$

could be investigated, where Q_0, Q_1, and Q_2 indicate three tensor polarizations depending on polarization direction [6,20]. In particular, we investigate the tensor-polarization asymmetry

$$A_{UQ_0} = \frac{1}{2\langle\sigma\rangle}\left[\sigma(\bullet, 0_L) - \frac{\sigma(\bullet, +1_L) + \sigma(\bullet, -1_L)}{2}\right], \quad (15)$$

in this work. Here, $\bullet$ indicates the unpolarized proton.

The Drell-Yan cross sections and spin asymmetries can be expressed in terms of PDFs. As shown in Fig. 5, the leading contribution to the hadron tensor is generally given by quark and antiquark correlation functions as

$$W_{\mu\nu}^{q\bar{q}} = \frac{1}{3}\sum_{a,b}\delta_{b\bar{a}}e_a^2\int d^4k_a d^4k_b\delta^4(k_a + k_b - Q) \times {\rm Tr}[\Phi_{a/p}(P_1S_1; k_a)\gamma_\mu\bar{\Phi}_{b/d}(P_2S_2; k_b)\gamma_\nu], \quad (16)$$

where k_a and $k_b = k_{\bar{a}}$ are quark and antiquark momenta, the color average and summations are taken by $3 \cdot (1/3)^2$, and the correlation functions $\Phi_{a/p}$ and $\bar{\Phi}_{\bar{a}/d}$ are defined by the quark field ψ as

$$(\Phi_{a/p})_{ij} = \int \frac{d^4\xi}{(2\pi)^4} e^{ik_a\cdot\xi} \langle P_1 S_1 | \bar{\psi}_j^{(a)}(0) \psi_i^{(a)}(\xi) | P_1 S_1 \rangle,$$
$$(\bar{\Phi}_{\bar{a}/d})_{ij} = \int \frac{d^4\xi}{(2\pi)^4} e^{ik_{\bar{a}}\cdot\xi} \langle P_2 S_2 | \psi_i^{(a)}(0) \bar{\psi}_j^{(a)}(\xi) | P_2 S_2 \rangle. \quad (17)$$

Here, link operators for satisfying the gauge invariance are not explicitly written. The correlation functions are expressed by unpolarized, longitudinally polarized, and transversity distributions and new tensor-polarized distributions. There is another contribution obtained by exchanging the quark and antiquark ($W_{\mu\nu}^{\bar{q}q}$).

Now, we express the Drell-Yan cross section, structure functions, and the tensor-polarization asymmetry in the parton model. There are 19 structure functions for the proton-deuteron Drell-Yan in the parton model; however, the number becomes four after the integration over the transverse momentum of Q. Denoting $\bar{F} = \int d^2 Q_T F$ for the structure function F, we have the pd Drell-Yan cross section [6],

$$\frac{d\sigma}{dx_1 dx_2 d\Omega} = \frac{\alpha^2}{4Q^2}\left[(1+\cos^2\theta)\left\{\bar{W}_T + \frac{1}{4}\lambda_1\lambda_2 \bar{V}_T^{LL} + \frac{2}{3}(2|\vec{S}_{1T}|^2 - \lambda_1^2)\bar{V}_T^{UQ_0}\right\} + \sin^2\theta |\vec{S}_{1T}||\vec{S}_{2T}| \cos(2\phi - \phi_1 - \phi_2)\bar{U}_{2,2}^{TT}\right], \quad (18)$$

where θ and ϕ are polar and azimuthal angles of the vector $\vec{k}_1 - \vec{k}_2$ for the dimuon, λ_1 and λ_2 are proton and deuteron helicities, and $\vec{S}_{1T}$ and $\vec{S}_{2T}$ are the transverse spin vectors for the proton and deuteron defined by the angles ϕ_1 and ϕ_2 as $\vec{S}_{1T} = |\vec{S}_{1T}|(\cos\phi_1, \sin\phi_1, 0)$ and $\vec{S}_{2T} = |\vec{S}_{2T}|(\cos\phi_2, \sin\phi_2, 0)$. The variables x_1 and x_2 are light-cone momentum fractions for the partons in the proton and deuteron, respectively. Neglecting hadron masses and transverse momentum of the dimuon, we have the relation $Q^2 = M_{\mu\mu}^2 = x_1 x_2 s$ [29]. The rapidity of the muon pair is given by $y = (1/2)\ln((E_{\mu\mu} + P_{\mu\mu,L})/(E_{\mu\mu} - P_{\mu\mu,L})) = (1/2)\ln(x_1/x_2)$, where $E_{\mu\mu}$ and $P_{\mu\mu,L}$ are the dimuon energy and longitudinal momentum. The momentum fractions x_1 and x_2 are expressed by these external variables as $x_1 = \sqrt{\tau}e^y$ and $x_2 = \sqrt{\tau}e^{-y}$. The dimuon transverse momentum is generally small in comparison with the dimuon mass in the Fermilab experiment [24]. In the parton model, the structure functions are expressed by the parton distributions for the process $q + \bar{q} \to \mu^+ + \mu^-$ as

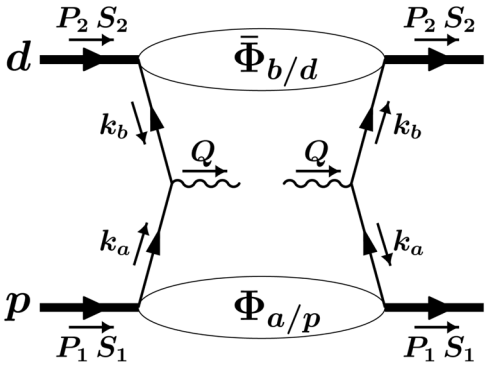

FIG. 5. Parton model for Drell-Yan process.

$$\bar{W}_T = \frac{1}{3}\sum_i e_i^2 q_i(x_1, Q^2)\bar{q}_i(x_2, Q^2) + (q \leftrightarrow \bar{q}),$$
$$\bar{V}_T^{LL} = -\frac{4}{3}\sum_i e_i^2 \Delta q_i(x_1, Q^2)\Delta\bar{q}_i(x_2, Q^2) + (q \leftrightarrow \bar{q}),$$
$$\bar{U}_{2,2}^{TT} = \frac{1}{3}\sum_i e_i^2 \Delta_T q_i(x_1, Q^2)\Delta_T\bar{q}_i(x_2, Q^2) + (q \leftrightarrow \bar{q}),$$
$$\bar{V}_T^{UQ_0} = \frac{1}{6}\sum_i e_i^2 q_i(x_1, Q^2)\delta_T\bar{q}_i(x_2, Q^2) + (q \leftrightarrow \bar{q}), \quad (19)$$

where Δq_i and $\Delta_T q_i$ are longitudinally polarized and transversity distributions. The terms $(q \leftrightarrow \bar{q})$ indicate the contributions from $\bar{q}(\text{in p}) + q(\text{in d}) \to \mu^+ + \mu^-$ by the replacements $q \leftrightarrow \bar{q}$ in the first terms.

In this article, we are interested in investigating the tensor-polarization asymmetry A_{UQ_0} of Eq. (15), and it is expressed in the parton model as [6,20]

$$A_Q \equiv 2A_{UQ_0} = \frac{2\bar{V}_T^{UQ_0}}{\bar{W}_T} = \frac{\sum_i e_i^2 [q_i(x_1, Q^2)\delta_T\bar{q}_i(x_2, Q^2) + \bar{q}_i(x_1, Q^2)\delta_T q_i(x_2, Q^2)]}{\sum_i e_i^2 [q_i(x_1, Q^2)\bar{q}_i(x_2, Q^2) + \bar{q}_a(x_1, Q^2) q_i(x_2, Q^2)]}, \quad (20)$$

where the factor of 2 is multiplied to define A_Q [25] so that the asymmetry becomes the simple ratio of the unpolarized PDFs $f(x)$ and the tensor-polarized PDFs $\delta_T f(x)$, although there is nothing wrong in the formalism of Ref. [6]. The scale Q^2 is given by the dimuon mass $Q^2 = M_{\mu\mu}^2 = (k_1 + k_2)^2 = (k_a + k_b)^2 = x_1 x_2 s$, and the unpolarized PDFs $f(x, Q^2)$ and tensor-polarized PDFs $\delta_T f(x, Q^2)$ should be obtained at this Q^2 scale for estimating the

asymmetry A_Q. The unpolarized PDFs are well known, and we could use the available parametrization for the tensor-polarized PDFs in Eq. (9) and Fig. 3 for our numerical calculations of A_Q.

III. RESULTS

Because the tensor-polarized PDFs are obtained at $Q^2 = 2.5$ GeV^2 in Eq. (9), they need to be evolved to the Q^2 points of the Fermilab Drell-Yan experiment. The proton beam energy is $E_p = 120$ GeV for the Fermilab Main Injector (MI), so the center-of-mass energy squared is $s = (p_1 + p_2)^2 = M_p^2 + M_d^2 + 2M_d E_p$ in the proton-deuteron Drell-Yan process with the proton (deuteron) 4-momentum p_1 (p_2) and its mass M_p (M_d). Then, the dimuon mass $M_{\mu\mu}$, which is equal to Q^2, is given by $Q^2 = M_{\mu\mu}^2 = x_1 x_2 s$. So far, the dimuon-mass region of $4^2\,\text{GeV}^2 < M_{\mu\mu}^2 < 9^2\,\text{GeV}^2$ is measured between the J/ψ and Υ resonances. Therefore, the Q^2 evolution of the tensor-polarized PDFs is necessary for estimating the tensor-polarization asymmetry for the Fermilab experiment.

A. Scale dependence of the tensor-polarized parton distribution functions

The Q^2 evolution of b_1 and the tensor-polarized PDFs is rarely discussed, so we briefly mention it here along the lines of the explanation of Ref. [3]. The operator product expansion (OPE) was studied within the twist-2 level, and the time-ordered product of two electromagnetic currents is expressed by twist-2 vector and axial-vector operators, $O_V^{\mu_1\cdots\mu_n}$ and $O_A^{\mu_1\cdots\mu_n}$. The vector operators are defined by the quark field ψ and the covariant derivative D^μ as

$$O_V^{\mu_1\cdots\mu_n} = \frac{1}{2}\left(\frac{i}{2}\right)^{n-1} S\left[\bar{\psi}\gamma^{\mu_1}\overleftrightarrow{D}^{\mu_2}\cdots\overleftrightarrow{D}^{\mu_n} e_q^2 \psi\right], \quad (21)$$

where S indicates the symmetrization of the indices $(\mu_1\ldots\mu_n)$ and removal of the trace. The structure functions $F_{1,2}$ and $b_{1,2}$ can be obtained from the vector operators $O_V^{\mu_1\cdots\mu_n}$, the matrix elements of which are expressed as

$$\langle p, E|O_V^{\mu_1\cdots\mu_n}|p, E\rangle = S\left[a_n p^{\mu_1}\ldots p^{\mu_n} + d_n\left(E^{*\mu_1}E^{\mu_2} - \frac{1}{3}p^{\mu_1}p^{\mu_2}\right)p^{\mu_3}\ldots p^{\mu_n}\right]. \quad (22)$$

The coefficients a_n and d_n are associated with the structure functions F_1 and b_1, respectively. Therefore, as explained in Ref. [3], the b_1 and b_2 are obtained from the same vector operators $O_V^{\mu_1\cdots\mu_n}$. Then, their anomalous dimensions and also coefficient functions in the OPE are common in $F_{1,2}$ and $b_{1,2}$, so the Q^2 evolutions of $b_{1,2}$ are the same as the ones for $F_{1,2}$. Namely, the Q^2 evolution of the tensor-polarized PDFs is calculated by the same Dokshitzer-Gribov-Lipatov-Altarelli-Parisi (DGLAP) evolution equations with the replacement of the unpolarized PDFs by the tensor-polarized PDFs. Therefore, the DGLAP Q^2-evolution code, for example in Ref. [30], can be used for calculating Q^2 variations of the tensor-polarized PDFs.

The tensor-polarized PDFs in Eq. (9) and Fig. 3 at $Q^2 = 2.5\,\text{GeV}^2$ are evolved to the Q^2 points, $Q^2 = M_{\mu\mu}^2 = x_1 x_2 s$, for the Fermilab MI kinematics by the standard DGLAP evolution equations [30]. At the initial scale of $Q_0^2 = 2.5$ GeV^2, the tensor-polarized charm and gluon distributions are assumed to be zero: $\delta_T c(x, Q_0^2) = \delta_T \bar{c}(x, Q_0^2) = \delta_T g(x, Q_0^2) = 0$. The uncertainties of the evolved PDFs are shown by the bands for $\Delta\chi^2 = 1$, and the uncertainty of the gluon distribution is also estimated. The evolution results of the set-2 tensor-polarized PDFs are shown in Fig. 6 from the initial $Q^2 = 2.5$ GeV^2 to $Q^2 = 30$ GeV^2, which roughly corresponds to a typical Q^2 value of the Fermilab experiment. Within this Q^2 variation, the PDFs do not change significantly, although the node position moves from $x = 0.22$ to 0.16. However, it is interesting to find a significant tensor-polarized gluon distribution $\delta_T g(x)$ due to the Q^2 evolution although it is zero in the initial scale, and its x dependence is much different from the quark and antiquark distributions. We use the evolution results at $Q^2 = x_1 x_2 s$ for given x_1 and x_2 for calculating the tensor-polarized spin asymmetries at Fermilab in the next subsection. For comparison, the evolution results of the set-1 tensor-polarized PDFs are shown in Fig. 7. Here, there is no antiquark tensor polarization at the initial scale $Q^2 = 2.5$ GeV^2. Finite tensor-polarized antiquark distributions are obtained at $Q^2 = 30$ GeV^2 due to the Q^2 evolution; however, they are still tiny as shown in the figure. Because the Drell-Yan

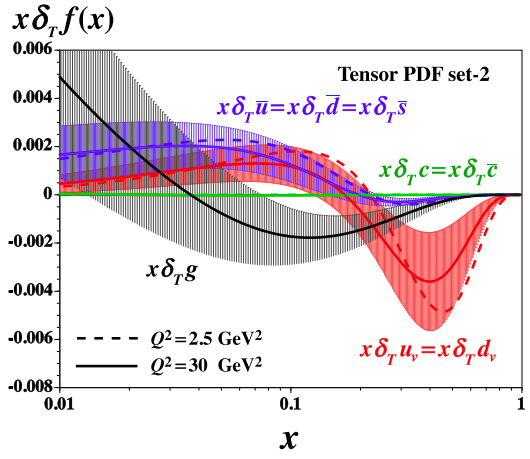

FIG. 6. Q^2 evolution results of set-2 tensor-polarized PDFs are shown. The dashed curves are the initial distributions at $Q^2 = 2.5$ GeV^2, and the solid curves indicate the tensor-polarized PDFs at $Q^2 = 30$ GeV^2.

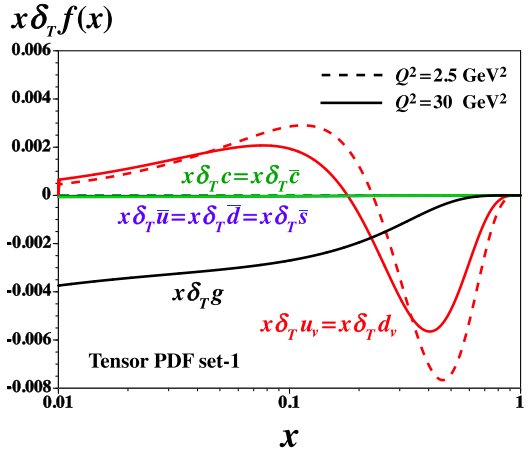

FIG. 7. Q^2 evolution results of set-1 tensor-polarized PDFs are shown. The dashed curves are the initial distributions at $Q^2 = 2.5$ GeV^2, and the solid curves indicate the tensor-polarized PDFs at $Q^2 = 30$ GeV^2.

cross section is sensitive to the antiquark distributions, it leads to small tensor-polarization asymmetries. At this stage, the set-2 distributions are more realistic ones because they can explain the HERMES measurements. It is also interesting to find a significant tensor-polarized gluon distribution although the antiquark distributions are very small in the set-1 parametrization.

B. Tensor-polarization asymmetry in proton-deuteron Drell-Yan process

We show the obtained tensor-polarization asymmetries A_Q in Fig. 8 at $x_1 = 0.2$, 0.4, and 0.6. There are two sets of tensor-polarized PDFs as shown in Eq. (9) and Fig. 3. The tensor-polarized PDFs are evolved from $Q^2 = 2.5$ GeV^2 to the scale $Q^2 = M_{\mu\mu}^2 = x_1 x_2 s$ by taking the proton energy

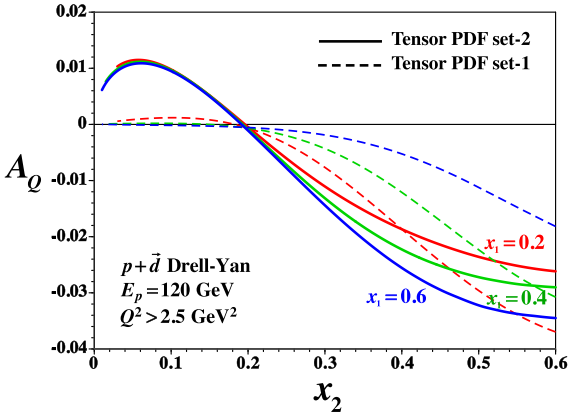

FIG. 8. Tensor-polarization asymmetries A_Q are shown for $x_1 = 0.2$, 0.4, and 0.6 by using two sets of tensor-polarized PDFs. The dashed curves are for the set 1 without the tensor-polarized antiquark distributions at the initial scale ($Q^2 = 2.5$ GeV^2), and the solid curves indicate the set-2 results.

$E_p = 120$ GeV with the fixed-target deuteron for the Fermilab MI experiment. Since the MSTW2008 unpolarized leading-order (LO) PDFs were used in the b_1 analysis [18], the MSTW2008-LO code [31] is used for calculating the unpolarized PDFs at the same Q^2 points. There are small nuclear corrections, usually within a few percent, in the unpolarized PDFs for the deuteron [32], but they are neglected in this work. In showing the curves, the experimental kinematical cut $4^2 < M_{\mu\mu}^2 < 9^2$ GeV^2 is not applied except for the condition $Q^2 = M_{\mu\mu}^2 > 2.5$ GeV^2. If x_1 is large, the large-x_2 region cannot be reached in the Fermilab experiment because of the condition $4^2 < M_{\mu\mu}^2 < 9^2$ GeV^2.

We find in Fig. 8 that the tensor-polarization asymmetry A_Q is generally of the order of a few percent. The set-1 asymmetries are rather small because the antiquark tensor polarization does not exist at $Q^2 = 2.5$ GeV^2, and it appears only by the Q^2 evolution. The set-2 asymmetries are generally much larger. We believe that the set-2 results are more reliable at this stage because they can explain the HERMES measurements including the small-x region as shown in Fig. 2. Since the HERMES b_1 data are taken in the region $0.012 < x < 0.452$, our predictions should be reasonable ones for the symmetries in the Fermilab experiment, where the kinematical region $0.1 < x_2 < 0.5$ will be probed. There are large differences in asymmetries between set 1 and set 2. However, in other words, it indicates the importance of measuring tensor-polarization asymmetry because it is the advantage of the Drell-Yan experiment to probe the antiquark distributions. Shadowing effects are effectively included in the HERMES data at small x, possibly at $x < 0.05$, and our predictions include such effects in set 2. However, the Fermilab experiment is not sensitive to the small x_2 region ($x_2 < 0.05$), so we may wait for the electron-ion collider project [23] for small-x measurements to probe shadowing effects on b_1.

One thing we need to check is the uncertainty of the tensor-polarized PDFs in showing the asymmetries because they are not well determined as shown in Figs. 3 and 6. We show the uncertainties for set 2 at fixed $M_{\mu\mu}^2 = Q^2 = 30$ GeV^2 in Fig. 9. There are large differences in the asymmetries between set 1 and set 2; however, they are mostly within the error bands, whereas the set-1 curve at small $x_2 (< 0.2)$ is outside of the $\Delta\chi^2 = 1$ band. This small-x_2 discrepancy is caused by the difference in handing the antiquark distributions at $x < 0.2$ originally in Fig. 3. Although the error bands are large, we predict a finite tensor-polarized asymmetry which could be investigated at Fermilab or other hadron facilities.

In Eq. (8), we mentioned that tensor-polarized antiquark distributions are important to measure for finding a possible mechanism on the tensor structure in quark and gluon degrees of freedom. Therefore, the Drell-Yan measurement is a valuable experiment which is very likely to create a new

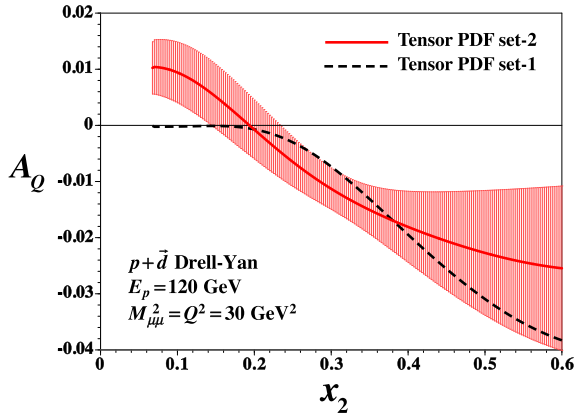

FIG. 9. Tensor-polarization asymmetries A_Q are shown at the fixed $M^2_{\mu\mu} = Q^2 = 30$ GeV^2 by using two sets of tensor-polarized PDFs. The dashed curve is for set 1 without the tensor-polarized antiquark distributions at the initial scale ($Q^2 = 2.5$ GeV^2), and the solid curve indicates the set-2 results. The uncertainty band is shown for the set-2 curve.

field of hadron physics. It is complementary to the JLab b_1 experiment, which will start in a few years. There is also a plan to measure the tensor polarization A_{zz} at JLab in the large-x region [22], and b_1 could be measured at the EIC [23].

Historically, the Fermilab Drell-Yan experiment played a crucial role in establishing the flavor asymmetric antiquark distributions $\bar{u} \neq \bar{d}$ [19]. This flavor asymmetry was suggested in the New Muon Collaboration (NMC) experiment by the violation of the Gottfried sum rule; however, it was not obvious whether the NMC experiment could be interpreted by a small-x contribution without the flavor asymmetric distributions. This issue was clarified by the Fermilab Drell-Yan experiment on the cross section ratio $\sigma^{\rm DY}_{pd}/(2\sigma^{\rm DY}_{pp})$, which directly probed $\bar{u} \neq \bar{d}$. In the same way, the tensor-polarized Drell-Yan experiment should be valuable for probing the antiquark tensor polarization directly. Hopefully, such an experiment will be done at Fermilab. In addition, it could be done at any facilities with high-energy hadron beams such as Brookhaven National Laboratory-RHIC, CERN-COMPASS, Japan Proton Accelerator Research Complex [33], Gesellschaft für Schwerionenforschung-Facility for Antiproton and Ion Research, and Institute for High Energy Physics in Russia.

IV. SUMMARY

There exist new polarized structure functions for spin-1 hadrons such as the deuteron. In particular, the twist-2 structure functions b_1 and b_2 of charged-lepton DIS are expressed in terms of tensor-polarized PDFs. These functions could probe the peculiar nature of hadrons in the sense that they should vanish if the internal constituents are in the S wave and that HERMES b_1 measurements are much larger than the conventional deuteron-model estimate.

New accurate measurements are planned at JLab by the electron DIS with the tensor-polarized deuteron. Furthermore, a Fermilab Drell-Yan experiment is now under consideration with the fixed tensor-polarized deuteron target. For pursuing this experiment and allocating beam time at Fermilab, it is crucial to estimate the magnitude of a possible tensor-polarization asymmetry theoretically. Using the optimum tensor-polarized PDFs obtained by analyzing the HERMES data, we estimated the tensor-polarization asymmetry by considering the Fermilab kinematics. We found that the asymmetry A_Q is of the order of a few percent.

It is a small quantity; however, we believe that it is worth it for the measurement to find the physics mechanisms of tensor polarization in the parton level. Especially, the Drell-Yan experiment should provide important information on the tensor-polarized antiquark distributions. It could lead to a new field of high-energy spin physics to probe an exotic aspect in hadrons. Furthermore, we showed in our analysis that a finite tensor-polarized gluon distribution should exist, and it has never been studied experimentally. It is also an interesting future topic.

ACKNOWLEDGMENTS

The authors thank X. Jiang, D. Keller, A. Klein, and K. Nakano for communications on a possible Fermilab Drell-Yan experiment with the tensor-polarized deuteron and R. L. Jaffe for communications on the scale dependence of the tensor-polarized PDFs and b1. This work was supported by Japan Society for the Promotion of Science (JSPS) Grants-in-Aid for Scientific Research (KAKENHI) Grant No. JP25105010. Q.-T. S is supported by the MEXT Scholarship for foreign students through the Graduate University for Advanced Studies.

[1] J. Ashman *et al.* (European Muon Collaboration), Phys. Lett. B **206**, 364 (1988); Nucl. Phys. **B328**, 1 (1989).

[2] L. L. Frankfurt and M. I. Strikman, Nucl. Phys. **A405**, 557 (1983).

[3] P. Hoodbhoy, R. L. Jaffe, and A. Manohar, Nucl. Phys. **B312**, 571 (1989); R. L. Jaffe and A. Manohar, Nucl. Phys. **B321**, 343 (1989).

[4] T.-Y. Kimura and S. Kumano, Phys. Rev. D **78**, 117505 (2008).

[5] F. E. Close and S. Kumano, Phys. Rev. D **42**, 2377 (1990); the sum rule is based on the parton model explained in R. P. Feynman, *Photon-Hadron Interactions* (Westview, Boulder, 1998).

[6] S. Hino and S. Kumano, Phys. Rev. D **59**, 094026 (1999); **60**, 054018 (1999); S. Kumano and M. Miyama, Phys. Lett. B **479**, 149 (2000).

[7] A. Airapetian *et al.* (HERMES Collaboration), Phys. Rev. Lett. **95**, 242001 (2005).

[8] H. Khan and P. Hoodbhoy, Phys. Rev. C **44**, 1219 (1991).

[9] G. A. Miller, *Topical Conference on Electronuclear Physics with Internal Targets*, edited by R. G. Arnold (World Scientific, Singapore, 1990), p. 30; G. A. Miller, Phys. Rev. C **89**, 045203 (2014).

[10] N. N. Nikolaev and W. Schäfer, Phys. Lett. B **398**, 245 (1997); **407**, 453 (1997); J. Edelmann, G. Piller, and W. Weise, Z. Phys. A **357**, 129 (1997); K. Bora and R. L. Jaffe, Phys. Rev. D **57**, 6906 (1998).

[11] A. Bacchetta and P. J. Mulders, Phys. Rev. D **62**, 114004 (2000).

[12] A. Schäfer, L. Szymanowski, and O. V. Teryaev, Phys. Lett. B **464**, 94 (1999); K.-B. Chen, W.-H. Yang, S.-Y. Wei, and Z.-T. Liang, Phys. Rev. D **94**, 034003 (2016).

[13] E. R. Berger, F. Cano, M. Diehl, and B. Pire, Phys. Rev. Lett. **87**, 142302 (2001); A. Kirchner and D. Mueller, Eur. Phys. J. C **32**, 347 (2003); M. Diehl, Phys. Rep. **388**, 41 (2003); F. Cano and B. Pire, Eur. Phys. J. A **19**, 423 (2004); A. V. Belitsky and A. V. Radyushkin, Phys. Rep. **418**, 1 (2005).

[14] W. Detmold, Phys. Lett. B **632**, 261 (2006).

[15] V. Dmitrasinovic, Phys. Rev. D **54**, 1237 (1996).

[16] C. Best, M. Göckeler, R. Horsley, E.-M. Ilgenfritz, H. Perlt, P. Rakow, A. Schäfer, G. Schierholz, A. Schiller, and S. Schramm, Phys. Rev. D **56**, 2743 (1997).

[17] S. K. Taneja, K. Kathuria, S. Liuti, and G. R. Goldstein, Phys. Rev. D **86**, 036008 (2012).

[18] S. Kumano, Phys. Rev. D **82**, 017501 (2010).

[19] S. Kumano, Phys. Rep. **303**, 183 (1998); G. T. Garvey and J.-C. Peng, Prog. Part. Nucl. Phys. **47**, 203 (2001); J.-C. Peng and J.-W. Qiu, Prog. Part. Nucl. Phys. **76**, 43 (2014).

[20] S. Kumano, J. Phys. Conf. Ser. **543**, 012001 (2014).

[21] Proposal to Jefferson Lab PAC-38, PR12-11-110, J.-P. Chen *et al.* (2011), https://www.jlab.org/exp_prog/proposals/11/PR12-11-110.pdf; K. Slifer, Tensor Polarized Solid Target Workshop, JLab, Newport News, VA, March 10–12, 2014 (unpublished), http://www.jlab.org/conferences/tensor2014/.

[22] E. Long, M. Strikman, M. Sargsian, and W. Cosyn, Tensor Polarized Solid Target Workshop, JLab, Newport News, VA, March 10–12, 2014 (unpublished); Proposal to Jefferson Lab PAC43, PR12-15-005, E. Long *et al.* (2014).

[23] C. Weiss and N. Kalantarians, Tensor Polarized Solid Target Workshop, JLab, Newport News, VA, March 10-12, 2014 (unpublished); D. Boer *et al.*, arXiv:1108.1713; A. Accardi *et al.*, arXiv:1212.1701; J. L. Abelleira Fernandez *et al.*, J. Phys. G **39**, 075001 (2012).

[24] X. Jiang, D. Keller, A. Klein, and K. Nakano (private communication); for the ongoing Fermilab E-906/SeaQuest experiment, see http://www.phy.anl.gov/mep/drell-yan/; the polarized proton-deuteron Drell-Yan measurement is considered in the Fermilab E1039 experiment.

[25] The overall factor $1/2$ is introduced in b_1 as it is used in F_1 and g_1 in expressing them (F_1 and g_1) by the unpolarized or longitudinally polarized PDFs.

[26] B. L. Ioffe, V. A. Khoze, and L. N. Lipatov, *Hard Processes* (Elsevier, New York, 1984).

[27] For example, M. Hirai, S. Kumano, and N. Saito, Phys. Rev. D **69**, 054021 (2004); see also https://cern-tex.web.cern.ch/cern-tex/minuit/node33.html, http://pdg.lbl.gov/2015/reviews/rpp2015-rev-statistics.pdf.

[28] E. D. Courant, Report No. BNL-65606, 1998.

[29] R. D. Field, *Application of Perturbative QCD* (Addison-Wesley, Reading, MA, 1989).

[30] M. Miyama and S. Kumano, Comput. Phys. Commun. **94**, 185 (1996); see also M. Hirai, S. Kumano, and M. Miyama, Comput. Phys. Commun. **108**, 38 (1998); **111**, 150 (1998); **183**, 1002 (2012).

[31] A. D. Martin, W. J. Stirling, R. S. Thorne, and G. Watt, Eur. Phys. J. C **63**, 189 (2009).

[32] M. Hirai, S. Kumano, and M. Miyama, Phys. Rev. D **64**, 034003 (2001); M. Hirai, S. Kumano, and T.-H. Nagai, Phys. Rev. C **70**, 044905 (2004); **76**, 065207 (2007).

[33] S. Kumano, Int. J. Mod. Phys. Conf. Ser., **40**, 1660009 (2016); Workshop on Hadron Physics with High-Momentum Hadron Beams, Japan Proton Accelerator Research Complex, 2013 (unpublished), http://www-conf.kek.jp/past/hadron1/j-parc-hm-2013/; Workshop on Hadron Physics with High-Momentum Hadron Beams, Japan Proton Accelerator Research Complex, 2015 (unpublished), http://research.kek.jp/group/hadron10/j-parc-hm-2015/.